Cytotechnology (2019) 71:819–833
https://doi.org/10.1007/s10616-019-00325-2

ORIGINAL ARTICLE

Construction of cardiomyoblast sheets for cardiac tissue repair: comparison of three different approaches

Gökçe Kaynak Bayrak · Menemşe Gümüşderelioğlu

Received: 25 February 2019 / Accepted: 20 June 2019 / Published online: 24 June 2019

Abstract Recently, cell sheet engineering has emerged as one of the most accentuated approaches of tissue engineering and cardiac tissue is the pioneering application area of cell sheets with clinical use. In this study, we cultured rat cardiomyoblasts (H9C2 cell line) to obtain cell sheets by using three different approaches; using (1) thermo-responsive tissue culture plates, (2) high cell seeding density/high serum content and (3) ascorbic acid treatment. To compare the outcomes of three methods, morphologic examination, immunofluorescent stainings and live/dead cell assay were performed and the effects of serum concentration and ascorbic acid treatment on cardiac gene expressions were examined. The results showed that cardiomyoblast sheets were successfully obtained in all approaches without losing their integrity and viability. Also, the results of RT-PCR analysis showed that the types of tissue culture surface, cell seeding density, serum concentration and ascorbic acid treatment affect cardiac gene expressions of cells in cell sheets. Although three methods were succeeded, ascorbic acid treatment was found as the most rapid and effective method to obtain cell sheets with cardiac characteristics.

Keywords H9C2 cell line · Cardiac tissue · Cell sheet engineering · Ascorbic acid · Thermo-responsive surface

Introduction

Cardiovascular diseases especially myocardial infarction are the leading cause of death in developed countries. Mature cardiomyocytes have limited ability to divide and the number of stem/progenitor cells are not enough to regenerate the damaged tissue. Consequently, adult heart cannot have a full functional recovery making it one of the leading organ candidates for regenerative medicine (Cui et al. 2018). Many different approaches including cell therapy, tissue engineering, angiogenic therapies and gene therapy, have been used to repair the heart. In cell therapy that directly injected isolated cells, poor survival was observed and control of shape, size and location of injection site was difficult (Matsuda et al. 2007; Haraguchi et al. 2012). In order to overcome the problems and fabricate functional tissue-engineered organs "top-down" or "bottom-up" approaches have been investigated.

Electronic supplementary material The online version of this article (https://doi.org/10.1007/s10616-019-00325-2) contains supplementary material, which is available to authorized users.

G. Kaynak Bayrak · M. Gümüşderelioğlu (✉)
Bioengineering Department, Hacettepe University, Ankara, Turkey
e-mail: menemse@hacettepe.edu.tr; menemse@gmail.com

M. Gümüşderelioğlu
Chemical Engineering Department, Hacettepe University, Ankara, Turkey

Cell sheet engineering technology, a bottom-up approach, has been progressing rapidly without using tissue scaffolds. Therefore, strong host inflammatory reactions (fibrosis, macrophage and neutrophil activations), insufficient cell migration, oxygen, nutrients and metabolic waste diffusion can be prevented. Also, cell dense-tissues that can not be fabricated with biodegradable scaffolds, are obtained with cell sheet technology (Matsuda et al. 2007; Wei et al. 2012; Zhang et al. 2016). Other than these, cell sheet technology has other advantages: (1) cell-to-cell connections and surface extracellular matrix (ECM) proteins secreted by the cells are preserved, (2) cell sheets can be transplanted to damaged area without any sutures, (3) cell sheets have flexibility, they can be fragmented and then injected, so cells keep their phenotype and localization of the cells can be improved, (4) using multiple cell sources thick and complex heterogeneous tissues can be reconstituted in vitro by assembling sheets (Chen et al. 2007; Haraguchi et al. 2012; Yu et al. 2014; Guo et al. 2015; Zhang et al. 2016).

Cell sheets are mainly obtained by using commercial thermo-responsive tissue culture plates. In these plates, a temperature-responsive polymer, poly(N-isopropylacrylamide) (PIPAAm), grafted surface is used. PIPAAm and its copolymers show thermo-responsive hydrophobicity in aqueous solutions (Matsuda et al. 2007). At 37 °C polymer shows hydrophobic character and cells can adhere, and spread on the surface but by lowering the temperature below 32 °C, hydrophilicity increases and grafted polymer starts to swell thus cells detach from the surface in sheet form by mechanical force generated by swelling (Haraguchi et al. 2012). However, polymer grafting process is complicated, time-consuming and relatively expensive (Wei et al. 2012; Yu et al. 2014). Therefore, researchers have developed different techniques for cell sheet formation and harvesting; using magnetite nanoparticles and magnetic force (Shimizu et al. 2007), light-induced cell detachment method (Hong et al. 2013), ion-induced cell detachment method (Zahn et al. 2012), fibrin coated dishes (Itabashi et al. 2005), appropriate cell density and serum content (Yeh et al. 2014) and reactive oxygen species (ROS)-induced strategy (Koo et al. 2018). Another commonly used alternative approach is ascorbic acid (AA) treatment. However, research on mechanism of action is not satisfactory, so how ascorbic acid induce cell sheet formation remain unknown (Guo et al. 2015).

Transplantation of cell sheet grafts onto damaged hearts provides a significant healing in in vivo studies and clinical trials. So far, cell sheet fabrication has been applied to many types of cells for cardiac tissue engineering including cardiomyocytes (Furuta et al. 2006; Haraguchi et al. 2006; Sekine et al. 2011), skeletal myoblasts (Memon et al. 2005; Hata et al. 2006; Kondoh et al. 2006; Hoashi et al. 2009), cardiac stem cells (Dergilev et al. 2017, 2018), mesenchymal stem cells (Miyahara et al. 2006; Chen et al. 2007; Bel et al. 2010), embryonic stem cells (Bel et al. 2010), endothelial cells (Sekine et al. 2008) and induced pluripotent stem (iPS) cells (Kawamura et al. 2012). H9C2 cardiomyoblasts were originally derived from embryonic rat ventricular tissue. The cells do not have the beating ability but have the contraction and expansion function (Zhou et al. 2016). Although they can not beat, they share similarities with primary cardiomyocytes in terms of membrane morphology, g-signalling protein expression and electrophysiological properties (Watkins et al. 2011). Also, they have some signalling pathways, taking in differentiation into mature cardiac muscle cells (Witek et al. 2016). Therefore, they are used in many studies including cardiotoxicity (Feridooni et al. 2013; Law et al. 2013; Witek et al. 2016), cardiac tissue engineering (Martinez et al. 2010; Cui et al. 2014) and heart disease (Jadaun et al. 2018; Tao et al. 2018) as an in vitro model. But H9C2 cells have not been used in cell sheet engineering studies yet.

In the present study, for the first time H9C2 cardiomyoblast sheets were obtained. We used three different techniques; (1) using thermo-responsive tissue culture plates, (2) inoculation with high cell density and serum content and (3) using ascorbic acid treatment on H9C2 cell sheet formation and harvesting of cell sheets. The characteristics of cell sheets were determined by means of morphologic observations, immunofluorescent staining, live/dead assay and Real-Time Polymerase Chain Reaction (RT-PCR) analysis. The results were evaluated by the need of the development of cardiac patch or graft.

Materials and methods

Materials

H9C2 rat cardiomyoblast cell line was kindly provided by Prof. Dr. Belma Turan (Ankara University, Faculty

of Medicine, Department of Biophysics, Turkey). Thermo-responsive tissue culture plates (35 mm in diameter) were purchased from UpCell® Thermo Fisher Scientific™ (USA). L-ascorbic acid was obtained from Sigma (Germany). For cell culture studies, Dulbecco's modified Eagle medium (DMEM) and fetal bovine serum (FBS) were obtained from Biowest (France). Dulbecco's phosphate buffer solution (DPBS) was purchased from Lonza (Switzerland). Trypsin/EDTA (0.25%) solution, penicillin–streptomycin and bovine serum albumin (BSA) were obtained from Sigma (Germany). Ethidium homodimer I and calcein-AM were purchased from Sigma (Germany). Alexa Fluor® phalloidin 488, a filamentous actin (F-actin) probe and DAPI (diamidino-2-phenylindole) were obtained from Invitrogen (USA) and Thermo Scientific (USA), respectively. MTT [3-(4,5-dimethylthiazol-2-yl)-2,5-diphenyltetrazolium bromide], which is used for cell viability analysis, was obtained from Sigma-Aldrich (Germany). Trizol used for RNA isolation was obtained from Invitrogen (USA).

Methods

Cell culture studies and fabrication of cell sheets

H9C2 cells were cultured in DMEM (4.5 g/L glucose) supplemented with 4 mM L-glutamine, 1% (v/v) penicillin/streptomycin and 10% (v/v) FBS under standard culture conditions (37 °C, 5% CO_2). Cells at the 20th passage were morphologically characterized by using crystal violet and immunofluorescence stainings. On the specified days of culture, the medium was removed and each well was washed with phosphate buffer saline (PBS, pH: 7.4). The cells were fixed in acetone-methanol solution (1:1, v/v) for 20 min. Then, the solution was removed and cells were treated with crystal violet solution for 30 min. After properly washing, images were captured using inverted microscope (Olympus IX71, USA). For immunofluorescence imaging, cells were fixed with 4% paraformaldehyde solution for 20 min at room temperature and permeabilized with 0.1% Triton-X-100 for 10 min. Then, sheets were stained with Alexa Fluor® phalloidin 488 (1:100) and DAPI (1:1000) in 1% BSA/PBS for 30 min at room temperature. After washing with PBS, cells were examined under the fluorescence microscope (Olympus IX71, USA). The proliferation and mitochondrial activity of the cells were determined using the MTT assay as described. After the culture medium was removed, MTT mix (600 µL culture medium and 60 µL MTT solution; 2.5 mg/mL in PBS) was added to each well and incubated for 3 h at 37 °C. Then, the mix was removed and precipitated formazan crystals were dissolved with 400 µL isopropanol (containing 0.04 M HCl) and optical density (OD) was measured using a microplate spectrophotometer (ASYS Hitech UVM 340 Plate Reader) at a wavelength of 570 nm with the reference to 690 nm. MTT assay and cell counting were performed on three samples (n = 3).

Cells were used at passage 26–28 in cell sheet studies. Three different methods were used to obtain cell sheets (Table 1). In the first method, thermo-responsive tissue culture plates were used and cells were seeded at 10^4 cells/cm^2 seeding density with 10% FBS containing medium. Culture medium was changed at 2–3 days intervals in all groups. At the 7th day of culture, commercial plates were cooled to 20 °C for 30 min and then, confluent cell sheets detached spontaneously. For second and third groups, 5×10^4 cells/cm^2 were seeded on 6-well TCPS (tissue culture polystyrene) plates with DMEM containing 20% (v/v) FBS. In the second group (high cell density/high serum content) cells were cultured for 9 days. After the culture period, medium was discharged and cells were washed with PBS twice. Then sheets were peeled off from the edges of the surface by gently washing with PBS. In the third method ascorbic acid was applied to the cultures in the presence of normal serum [10% (v/v), N-FBS] and high serum [20% (v/v), H-FBS] contents (Table 1). The effect of ascorbic acid on cell culture media pH was determined with pH measurements. The day after cell seeding, medium was changed with AA containing media in 3 different concentrations (20, 50 and 100 µg/mL AA) and cultures were continued until day 5. The AA concentrations were selected in accordance with the literature (Wei et al. 2012; Guo et al. 2015). Sheets were detached by using the same protocol that was used for the 2nd group. All obtained sheets were transferred to a new well by using simple pipetting as explained by Haraguchi et al. (2012). In order to prevent the sheets from drying completely, a few drops of medium were added until sheets completely adhered. Then 2 mL culture medium was added to each well and characterization studies were carried out.

Table 1 Three different methods used for obtaining H9C2 cell sheets

Methods	Cell seeding density (cells/cm^2)	FBS concentration (v/v %)	Detachment period (Day)	Ascorbic acid concentration (μg/mL)
Thermo-responsive plate	1×10^4	10	7	–
High cell density/FBS concentration	5×10^4	20	9	–
Ascorbic acid treatment	5×10^4	10	5	20; 50; 100
		20		

Characterization of cell sheets

All groups of cell sheets were morphologically observed under inverted microscope. Images were taken before/after detaching and after re-adhesion to new tissue culture plates. In order to view actin cytoskeleton and nucleus, sheets were stained with Alexa Fluor® 488 phalloidin and nuclei of the cells were counterstained with DAPI. Live/dead staining based on plasma membrane integrity and esterase activity was performed to investigate cell viability. After cultivation, sheets were submerged in a live/dead staining solution (2 μM calcein-AM and 2 μM ethidium homodimer-1) and incubated for 30 min at room temperature. Then, sheets were washed with PBS and images were acquired using a fluorescence microscope.

The effects of tissue culture surface material (TCPS or PIPAAm grafted surface), high (5×10^4 cells/cm^2) or low (1×10^4 cells/cm^2) cell seeding density and FBS concentration (10% or 20%) with ascorbic acid treatment on specific gene transcripts (collagen type I (*Col1a1*), cardiac type troponin T2 (*Tnnt2*), calcium voltage-gated channel subunit alpha1 C (cardiac type; *Cacna1c*) and alpha1 S (skeletal type; *Cacna1s*) and solute carrier family 29 member 1 (equilibrative nucleoside transporter-1; ENT-1; *Slc29a1*) were investigated with real time reverse transcriptase polymerase chain reaction (RT-PCR). Primer sequences were shown in supplementary Table I. In order to investigate the influence of seeding density (low or high), cells were cultured at 10^4 cells/cm^2 seeding density on a TCPS dish with 40 mm diameter. This was evaluated as both TCPS-surface control group versus thermo-responsive surface group and low cell seeding density group versus high cell density group.

For RT-PCR, cells were first trypsinized, centrifuged in Eppendorf tube and stored at − 80 °C until analysis. For RNA extraction, 500 μL Trizol was added to each sample and RNeasy Mini kit (Qiagen, Valencia, CA) was used. RNA concentration was determined by measuring optical density at 260 nm using Nanodrop 2000c (Thermo Scientific, USA). Then, cDNA was synthesized using a high-capacity cDNA kit (Applied Biosystems, USA) and RT-PCR reactions were performed with 5xHot Fire Pol® Eva Green® qPCR Mix Plus solution (Solis BioDyne, Estonia) and LightCycler® Nano Instrument (Roche, Germany). Glyceraldehyde 3-phosphate dehydrogenase (*Gapdh*) was used as a housekeeping gene and expressions were determined using the $2^{(-\Delta\Delta Ct)}$ method. The results were given as fold change relative to control group.

Statistical analysis

All the experiments were performed four times and data were expressed as mean ± standart deviation. Statistical analyses were performed using GraphPad InStat software and two tailed *t* test or One-way ANOVA was used to determine the significant differences among the groups and a statistical significance was assigned with *p* values.

Results

Rat cardiomyoblasts, H9C2, cells were cultured for characterization until day 14. Crystal violet and fluorescence staining images, indicating cells' myoblast morphology, were shown in Fig. 1a–f. Mitochondrial activity of the cells increased during the subsequent culture as seen in MTT graph (Fig. 1g). Doubling time and specific growth rate of cells were calculated as 54 h and 0.0128 h $^{-1}$, respectively.

General observation

In the first group we cultured H9C2 cells on temperature-responsive dishes for 7 days. Upon confluence, a continuous monolayer sheet was formed on the surface (Fig. 2a) and as the temperature decreased sheets started to detach within 15 min and floated up into the culture medium at the end of 30 min. In the second group, using high cell density/high serum content, we obtained a complete cell sheet without using any special equipment, but in longer time. In AA-treated group, we used 2 different FBS and 3 different AA concentrations and were able to obtain cell sheets within 5 days. Before treatment, pH values of the media were measured and it was seen that statistically there were not much changes between growth medium and ascorbic acid added media ($*p < 0.05$) in different ascorbic acid concentrations. After detachment, cells rounded up as seen in Figs. 2b, f and 3d–f. All sheets were easily transferred into new 6-well plates. After the re-adhesion, cells spreaded well again (Figs. 2c, g, d, h, 3g–i, 4f–h).

Immunofluorescent stainings

Before attachment and after re-adhesion, cell sheets were stained with fluorescence dyes to investigate the changes in cytoskeleton structure and nuclear

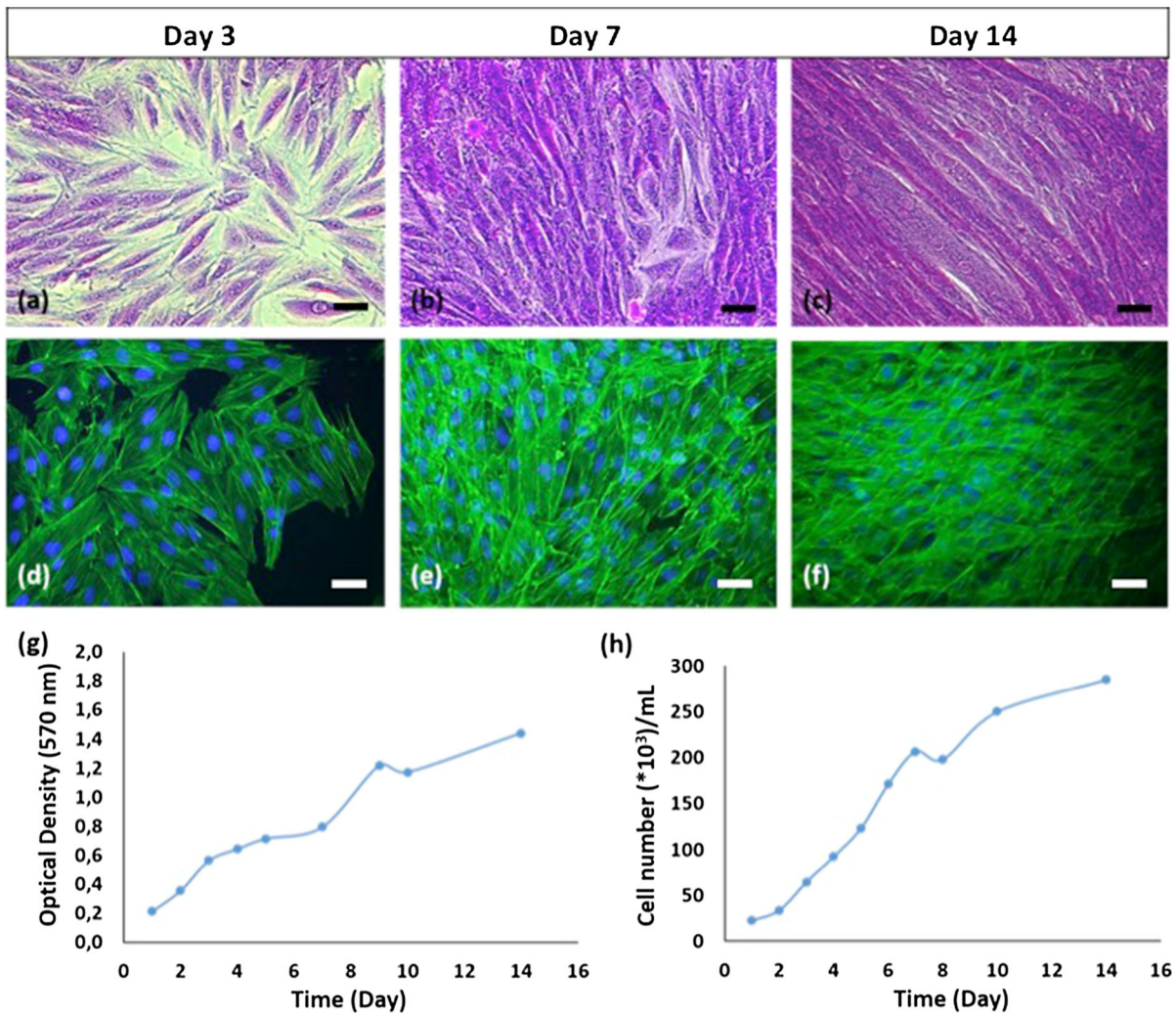

Fig. 1 H9C2 cells characterization studies. Crystal violet staining (**a**, **b**, **c**; 32X), immunofluorescence staining (**d**, **e**, **f**; 32X), MTT results (**g**), cell growth curve (**h**) of H9C2 cells (scale bars: 50 μm). (Color figure online)

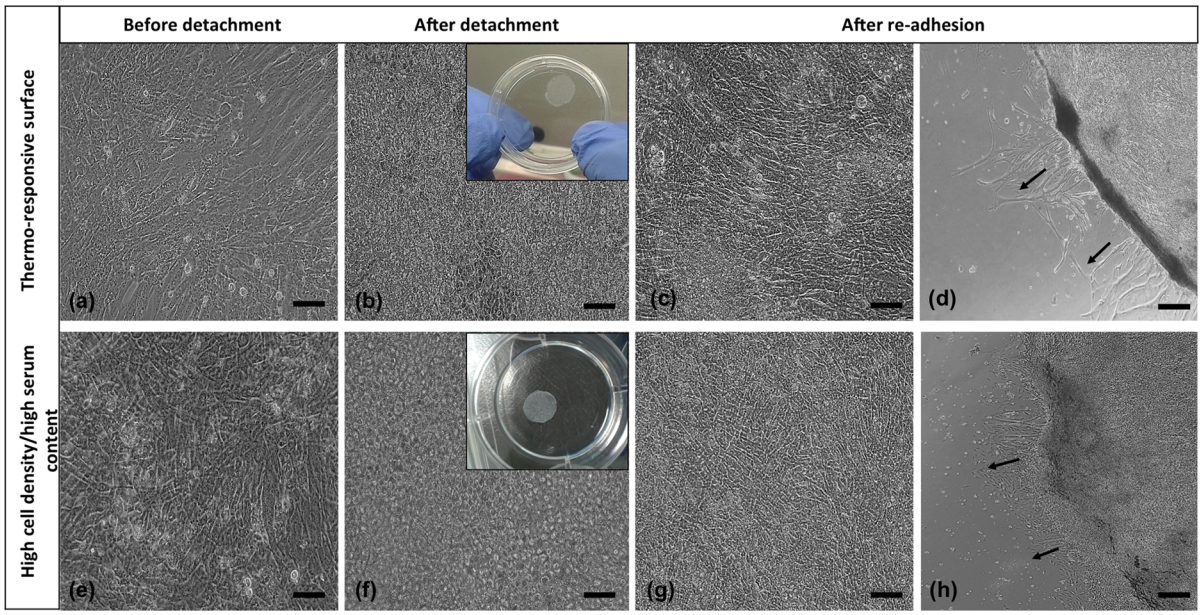

Fig. 2 The morphology of cell sheets obtained by thermo-responsive surface and high cell density/high serum content methods. **a**, **e** Before detachment (20X); **b**, **f** after detachment (20X); **c g** 3 days and 1 day after re-adhesion (20X); **d**, **h** 3 days and 1 day after re-adhesion (4X) (scale bars: 20X 100 µm; 4X 500 µm). Black arrows show sprouting of cells from cell sheets

morphology. Actin flaments (green) and nuclei (bright blue) were clearly observed in all sheets (Fig. 5). Especially in the high cell density/high serum content and AA-treated groups, F-actin, filaments appeared highly cross-linked because of high cell density and overlaping of cells within the sheets. Also, there was a significant increment in spindle-shape cell morphology with the use of AA and its increasing concentrations (Fig. 5d, e, f, j, k, l). Cell nuclei in all sheets exhibited round shape in bright blue colour but some fragmented nuclear residuals were seen in sheets having high cell density.

Live/dead stainings

Live/dead staining was performed to investigate whether the methods used for obtaining cell sheets have a negative effect on the cell viability. Live (green) and dead (red) cells were determined from the merged version of the fluorescence microscopy images (Fig. 6). The assay showed that in all groups cells have high vitality before detachment (Fig. 6a, c, d, e, f, j, k, l) and most of them survived after cell sheet detachment and re-adhesion (Fig. 6b, g, h, i, m, n, o).

RT-PCR analysis

The results of RT-PCR analysis were given in Fig. 7 and showed that PIPAAm surface modification increased only *Cacna1s* expressions (Fig. 7a). Seeding density affected gene expressions as well at low cell seeding density *Col1a1* increased but *Tnnt2* and *Cacna1s* expressions decreased (Fig. 7b). It was also shown that FBS concentrations and AA treatment had an important effect on ECM, skeletal and cardiac specific genes (Fig. 7c). Collagen type-1 expressions significantly increased in all AA treatment groups. Increased serum concentration enhanced the collagen expressions only in control and 100 µg/mL AA groups. In general, AA treated cell sheets showed decreased *Tnnt2* expressions. This decrease was more distinct in the H-FBS group. In addition, increased FBS concentration in 20 and 50 µg/mL AA groups negatively affected *Tnnt2* expression negatively. It was observed that AA addition did not make a significant difference in the expression of Slc29a1 gene. Significant increase was observed only in the 100 µg/mL AA group with high FBS. High FBS concentration increased *Cacna1c* expressions in all groups and *Cacna1s* expressions in all AA addition

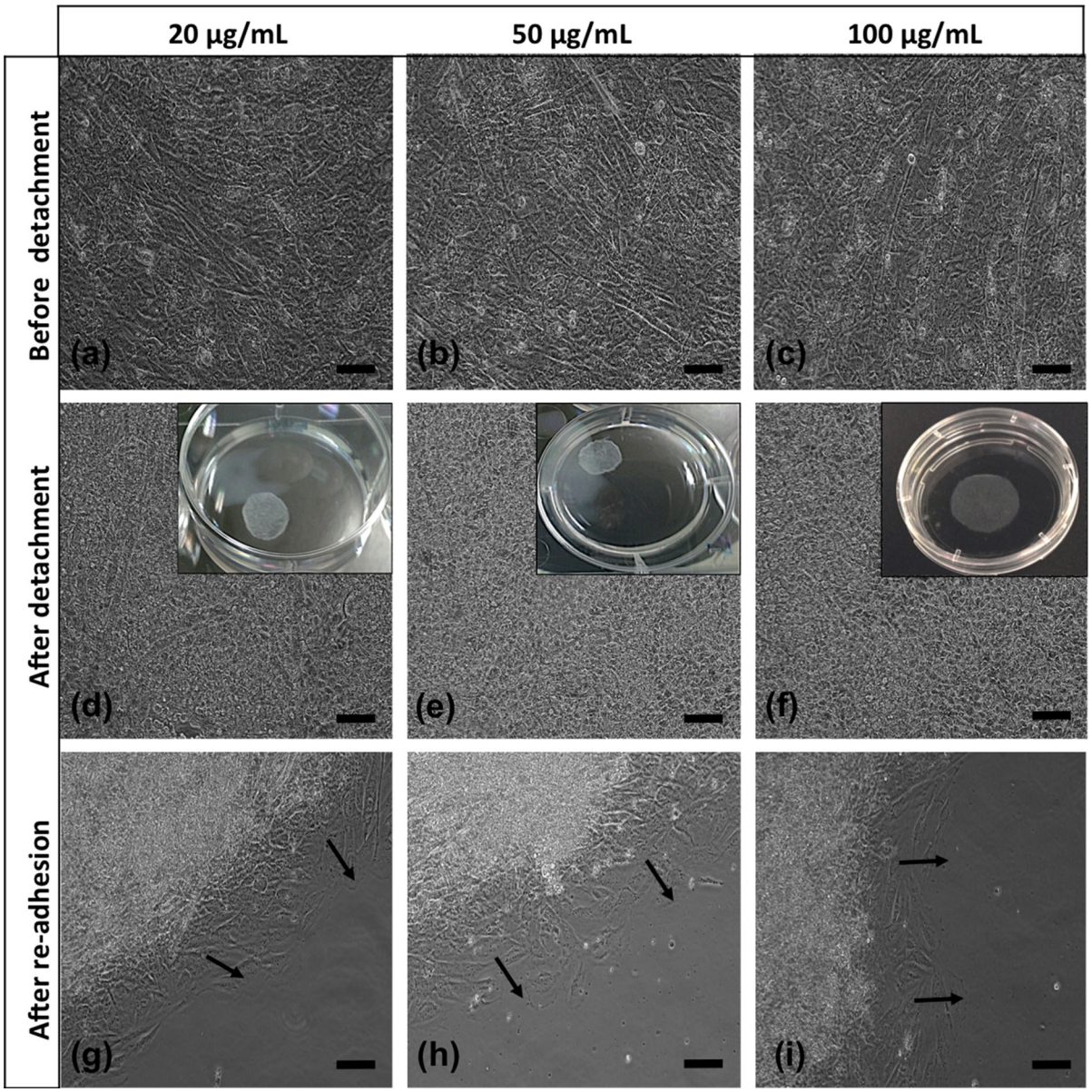

Fig. 3 Morphologies of AA-treated cell sheets with high serum content (20X, scale bars: 100 µm). Black arrows show sprouting of cells from cell sheets

groups. Also AA treatment stimulate *Cacna1s* expressions in both N-FBS and H-FBS groups.

Discussion

Cell seeded scaffolds are usually used in conventional tissue engineering although their numerious limitations. As an alternative approach, cell sheet engineering has been investigated. Natural cellular junctions and microenvironments will be provided. Although cell sheet applications have been investigated in cardiac tissue engineering, H9C2 cell line, have never been used in that application. We choose H9C2 cell line instead of primary cardiomyocytes because of their similarity to cardiomyocytes. Also primary cells have limited proliferation capacity and you do not need to sacrifice animals for each study

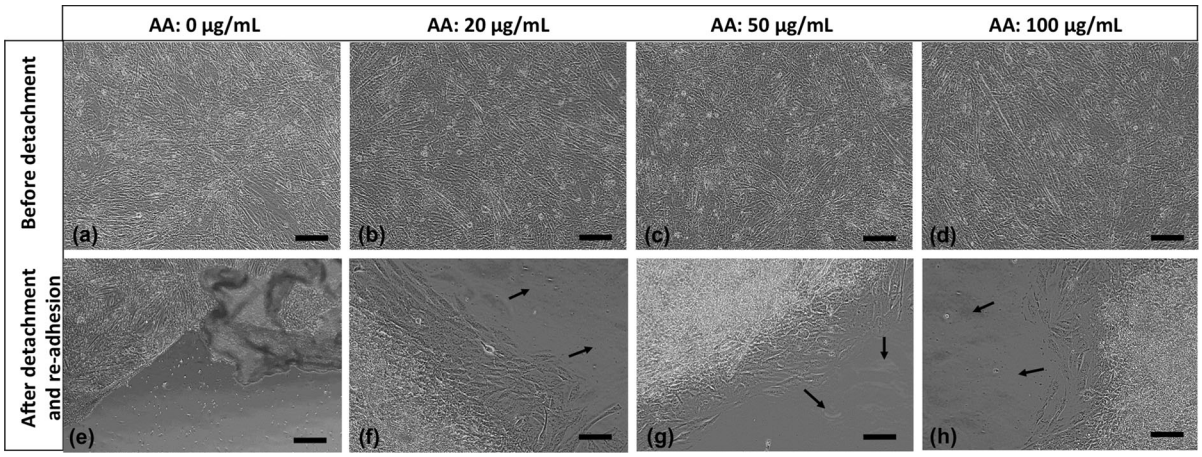

Fig. 4 Morphologies of AA-treated cell sheets with normal serum content (20X, scale bars: 100 µm). Black arrows show sprouting of cells from cell sheets

when you use the cell line. In this study, we compared three different procedures to obtain usable cardiomyoblast sheets by a simple, fast and efficient method.

The results of H9C2 cells characterization studies are in accordance with literature. As seen in Fig. 1 H9C2 cells have typical morphology of mononucleated and small spindle shaped myoblasts. At low densities the cells were randomly oriented, but in confluency they mostly organize themselves into linear configuration. MTT graph in Fig. 1g is in conformity with cell growth curve in Fig. 1h in terms of cell growth phases. Following exponential growth phase cells continued to proliferate at a slower speed until the end of the culture. As seen in Fig. 1b–c and e–f, cells coated culture surface completely on the 7th and 14th day. They started to squeeze after confluency, also they produce their own ECM and some cells can grow on this ECM. Thus, cells can proliferate a little more after they reached confluency. As the culture progress there will be no free space, therefore cells will enter the stationary and death phases, respectively. Doubling time of H9C2 cells was found compatible with the result which was indicated in the literature, approximately 54 h (Dott et al. 2014).

In the cell sheet studies, firstly we used commercial thermo-responsive dishes and obtained sheets without treating with any enzymes at the end of the 7th days of culture period. In the second method, we used high cell seeding density (5×10^4 cells/cm^2) and high serum content (20%) and cells were able to develop into sheet in 9 days since serum has stimulating effect on both cell growth and collagen synthesis (Narayanan et al. 1989). Also, its increasing concentrations enhance cell growth (Choi et al. 1980) and collagen synthesis (Kato et al. 1996). Therefore, using high FBS concentration induces proliferation and collagen synthesis to support cell sheet formation. Yeh et al., obtained adipose-derived stem cell sheet by a similar method and brief trypsinization (Yeh et al. 2014). Here we detached the sheets with only PBS washing, so sheets could be obtained without losing their integrity.

Recently, ascorbic acid (AA) treatment has been investigated for harvesting cell sheets. Adding AA to cell culture medium, increases collagen and ECM secretion of cells in a short time and ECM provides integrity and mechanical strength to the cell sheets. (Grinnell et al. 1989; L'Heureux et al. 1998; Zhang et al. 2016). Also, ECM includes various signals and arranges the interactions between soluble factors and cells. So, it plays an important role in tissue regeneration. Wei et al. used AA-treatment to induce the cell sheet formation of periodontal ligament stem cells, umbilical cord and bone marrow mesenchymal stem cells. They indicated that cells preserved not only tight cell-to-cell junctions and ECM, but also microfilaments and exocytotic vesicles near the plasma membrane, which implies high cellular activity by this method (Wei et al. 2012). Otherwise, AA induces cardiac differentiation of embryonic stem cells or iPSCs (Yu et al. 2014; Ivanyuk et al. 2015). AA has also been used as cell culture supplement to stimulate collagen production, DNA synthesis and suppress

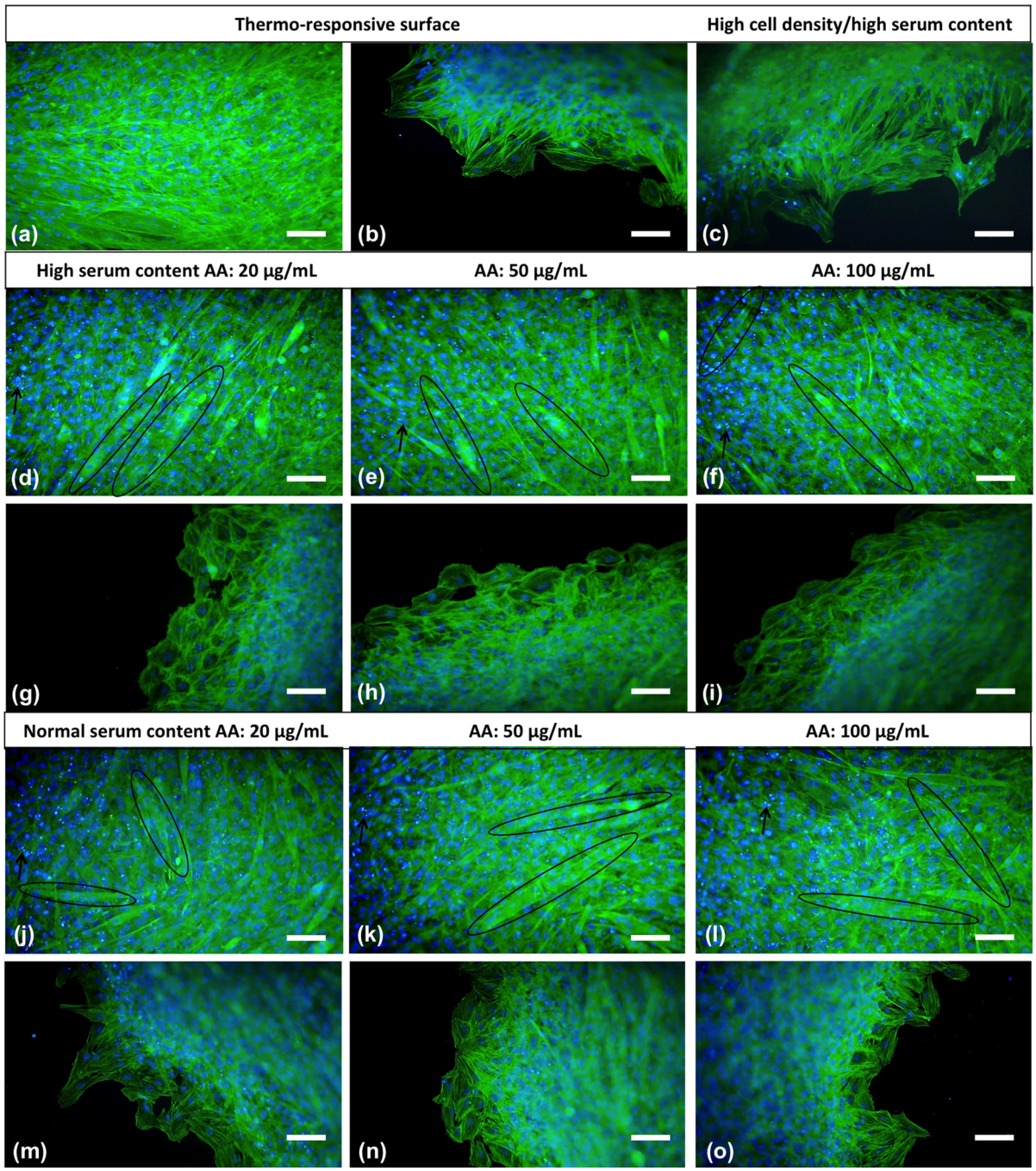

Fig. 5 Fluorescence staining of cell sheets obtained by thermo-responsive surface (**a**, **b**), high cell density/high serum content (**c**) and AA treatment (high serum content: **d**, **e**, **f**, **g**, **h**, **i**; normal serum content: **j**, **k**, **l**, **m**, **n**, **o**). Actin filaments and nuclei are green and bright blue coloured, respectively (20X, scale bars: 100 µm). (Color figure online)

intracellular reactive oxygen species (ROS) levels. Martinez et al., added AA into the culture medium of H9C2 cells and they emphasized that AA enhanced cells survival through inhibition of cell apoptosis. They also showed that viability and angiogenic potential of the engineered tissues in vivo are better with AA enrichment (Martinez et al. 2010). Huang et al. (2009), used AA as an antioxidant and showed its

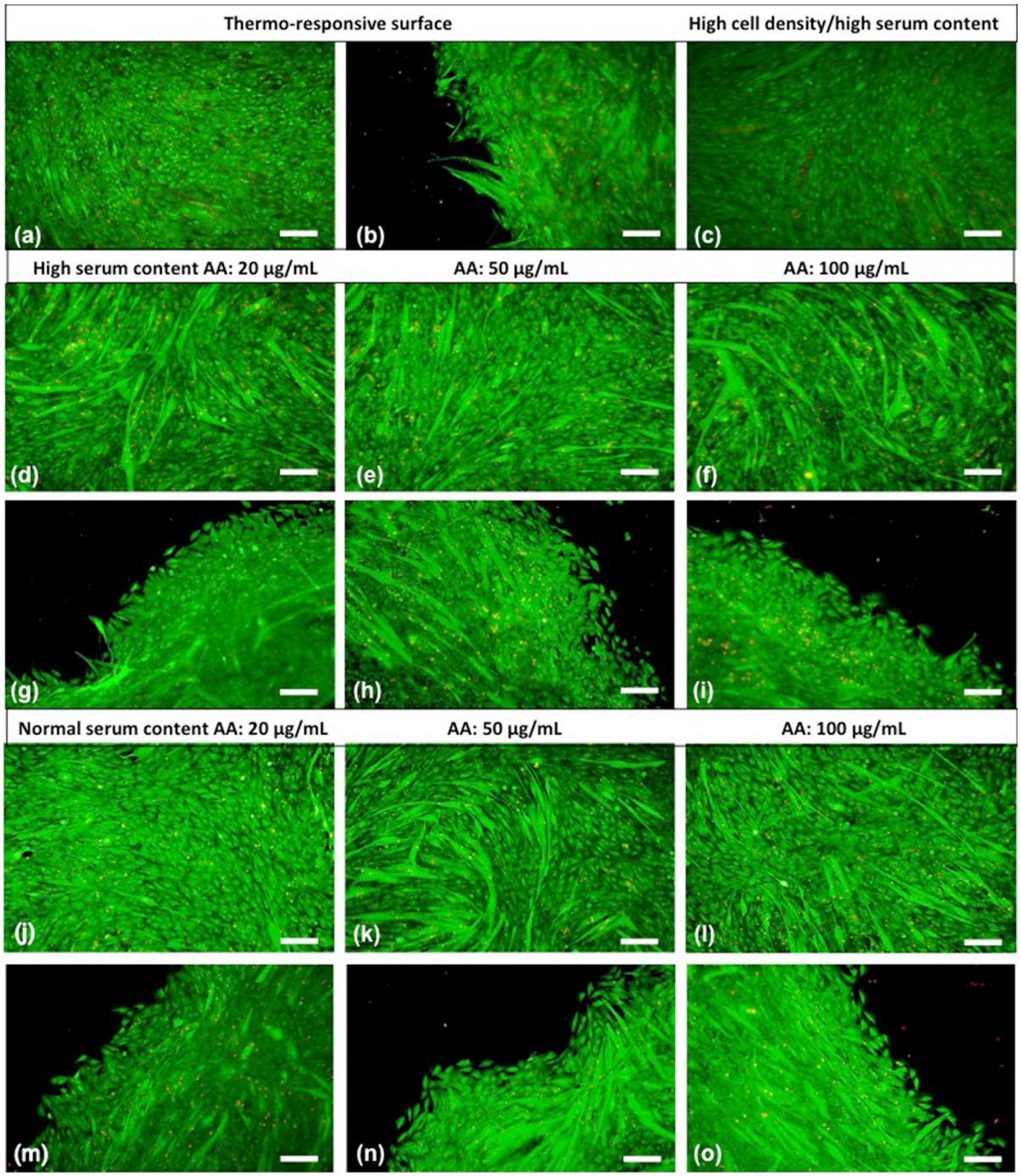

Fig. 6 Live/dead staining of cell sheets obtained by thermo-responsive surface (**a**, **b**), high cell density/high serum content (**c**) and AA treatment (high serum content: **d**, **e**, **f**, **g**, **h**, **i**; normal serum content: **j**, **k**, **l**, **m**, **n**, **o**). Live and dead cells are green and red coloured, respectively (10X, scale bars: 200 µm). (Color figure online)

diminishing effect of hypothermia-induced apoptosis. On the other hand, there are several studies on cytotoxic effects of AA with showing different concentrations have toxicity to different cell types such as 300 µg/mL AA or more on hyalocytes, 1 mM or more on human cell lines and tenocytes (Hakimi

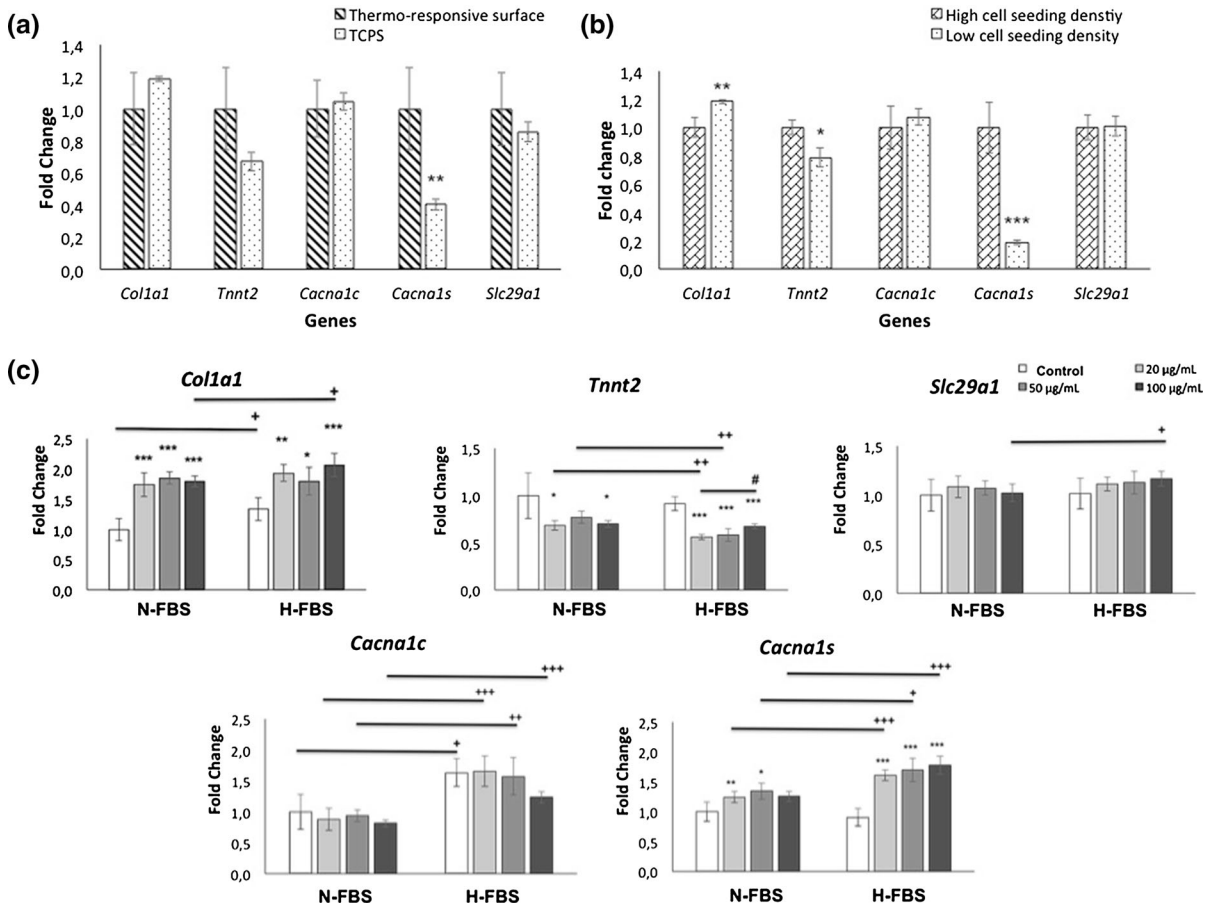

Fig. 7 RT-PCR analyses for *Col1a1*, *Tnnt2*, *Cacna1c*, *Cacna1s* and *Slc29a1* genes. Comparison of thermo-responsive and TCPS surface (**a**), high and low cell seeding density at TCPS (**b**) and AA treatment groups in two different FBS content (**c**). TCPS surface and low cell seeding density groups are the same. Statistically significant differences are denoted by symbols; **a**, **b** n = 4; $^{*}p < 0.05$, $^{**}p < 0.01$ and $^{***}p < 0.001$; **c** n = 5; N-FBS and H-FBS groups were compared according to control among themselves $^{*}p < 0.05$, $^{**}p < 0.01$ and $^{***}p < 0.001$, 20 µg/mL AA served as control $^{\#}p < 0.05$; N-FBS groups served as control versus H-FBS groups $^{+}p < 0.05$, $^{++}p < 0.01$, $^{+++}p < 0.001$

et al. 2014). Also, AA addition decreases the pH of the medium and this can affect cell viability, but in our study we used maximum ∼ 0.5 mM AA concentration and pH reduction was not so high and cells were not adversely affected.

Cells in thermo-responsive plate group showed the typical morphology of cultured H9C2 cardiomyoblasts (Fig. 2). But in other groups cells were more fusiform-shaped before detachment because of high seeding density (Figs. 2, 3 and 4). After detachment there was no substantial difference among three methods with regard to cell integrity. After transfer to the new plates the cells started to migrate in a couple of days. Sprouting of cells from cell sheets was shown with black arrows in the figures. So, these results demonstrated that H9C2 cells composing the sheets were still alive and healthy. Cell sheets created by AA-treatment were obtained in a shorter time period without any defect. There was no distinct difference among cells treated with different AA or FBS concentrations in morphologically and the sheets were of similar quality as the cell sheets derived from other two methods. Besides, sheets in AA-treatment groups especially in high serum content were more resistant to manipulation and had higher mechanical strength due to ascorbic acid addition.

H9C2 cells were stained with immunofluorescent dyes to investigate the nucleus and F-actin cytoskeleton (Fig. 5). There was not any significant difference in F-actin organizations and nuclear

morphology between cells that migrated from sheets to the culture plate and H9C2 cells cultured in standart culture conditions. There was not any fracture or change in the organization of the actin cytoskeleton of cells migrating from sheets after detachment and re-adhesion despite the centre section of the cell sheets were not observed clearly. In thermo-responsive plate group, cells were monolayer so nucleus of the cells were observed individually in contrast to imbricated nuclei in other groups. Condensation and apoptotic bodies were observed in some cells that undergoing apoptosis. Brighter and smaller DAPI stained nucleus fragments are indicator of apoptotic bodies and demonstrated with black arrows.

In addition, multinucleated cells were seen frequently in high cell density/high serum content and more in AA-treated sheets (shown in eliptical) (Fig. 5d, e, f, j, k, l). In thermo-responsive plate group, cells were mostly mononucleated in contrast to others (Fig. 5a, b). Increased spindle-shape cell morphology of AA-treatment group may be due to the boost effect of ascorbic acid on cell proliferation and collagen synthesis. So, crowded cells in AA treatment group fused and joined together to form myotube-like structure indicated in Fig. 5d, e, f and Ricotti et al. (2012) also showed myotube formation by nuclei and cytoskeletal actin fluorescence staining as we did. Optical microscope of H9C2 cells photograph of myotubes in high cell density/high serum content and AA-treated sheet (H-FBS, 20 µg/mL) were given in supplementary data (Fig. S1). Similar fused and multinucleated structures were seen in other AA-treated groups. The morphology of H9C2 cells switched from myoblast-like to elongated-like was also consistent with inverted microscope images.

In live/dead cell staining assay, it was shown that no. of dead cells increased with high cell seeding density and rising AA concentration due to cell compaction (Fig. 6). Additionally, more fused, elongated and acicular-shaped cells were seen in AA-treated cell sheets (Fig. 6d, e, f, j, k, l). Also, a great majority of cells migrated from sheets were healthy and alive. The results were compatible with immunofluorescent stainings.

In addition to these assays, RT-PCR analysis was performed to detect the influence of surface material of plate, high or low cell seeding density and different FBS concentrations with AA treatment on gene expressions of H9C2 cells (Fig. 7). H9C2 cells simultaneously express both skeletal (*Cacna1s*) and cardiac (*Cacna1c*) types of calcium voltage-gated channel subunit Alpha1 genes. *Cacna1s* and *Cacna1c* specifically correlate with skeletal muscle and cardiac differentiation, respectively (Menard et al. 1999). Skeletal type channel generates contractile activity in primary cardiac myocytes culture (Mejia-Alvarez et al. 1994). The expression levels of these genes increase or decrease according to the differentiation tendency of the cells. *Tnnt2* gene regulates production of troponin T protein that participate in contractions and is an important cardiac marker (Pereira et al. 2011). The *Slc29a1* gene is responsible for the production of equilibrative nucleoside transporter-1 (ENT-1) proteins, which are responsible for the transport of adenosine, that plays an important role in many physiological processes in H9C2 cells. The increase in ENT-1 gene expression is considered as an indicator of cardiac differentiation of the cells (Leung et al. 2007; Rodgers et al. 2009).

Compared to TCPS and PIPAAm coated surfaces, only *Cacna1s* gene was affected by PIPAAm coating and its expression was enhanced (Fig. 7a). Thermo-responsive dishes have small prickles on their grafted surface (Yamato and Okano 2004). These nano-topographic details have an impact on cell behaviour and differentiation trends. So, these details may have affected gene expression. Cell seeding density impressed gene expressions in a similiar manner by cell interactions (Fig. 7b). It has been shown in many studies that low cell density (reduced cell–cell contact) increases collagen synthesis (Kato et al. 1996). Our RT-PCR results support the findings in the related literature. *Tnnt2* gene expression decreased with low seeding density and this may be due to reduced cell interactions. Decreasing *Cacna1s* expressions was also compatible with other results and showed enhanced myoblastic character by higher cell density. Besides, FBS concentration and AA treatment had important impact on gene expressions. Collagen type 1 expressions were increased with AA treatment in all FBS groups as indicated in previous studies with periodontal ligament, bone marrow stem cells and fibroblast cells (Grinnell et al. 1989; Wei et al. 2012; Guo et al. 2015;). While related literature showed increased FBS has stimulating effect on collagen synthesis (Narayanan et al. 1989), in our study similiar results were obtained also in control and 100 µg/mL AA groups. Ascorbic acid has recently been

recognized as cardiogenesis-promoting molecule that stimulates cardiac differentiation of embryonic stem cells or induced pluripotent stem cells (Yu et al. 2014; Ivanyuk et al. 2015). But contrary, according to our results of RT-PCR analysis AA supplementation reduced *Tnnt2* gene expressions in most concentrations and did not affect *Slc29a1* and *Cacna1c* expressions, but increased *Cacna1s* expressions in all concentration. This impact may be due to high cell density influence on H9C2 cells was more dominant to effects of applied AA concentrations. Enhanced FBS concentration reduced Tnnt2 gene expression except the highest AA group. But increased *Slc29a1* expression of the highest AA concentration and *Cacna1c* expressions in all groups. Also promoted *Cacna1s* expressions in all AA treated groups probably based on inducing cell proliferation that cause cell squeezing. When all the results are evaluated, it can be concluded that AA induced myogenic characteristics of H9C2 cells by inducing *Cacna1s* gene expression and cell sheets having high cardiac characteristics can be obtained by using high FBS (20%) and AA concentration (μg/mL) together.

Conclusion

In native heart, cells are dense and tightly connected, so cell sheet engineering technology presents enormous potential for the creation of suitable engineered cardiac tissue. In this study, we demonstrated the successful construction of cardiomyoblast cell sheets without using thermo-responsive dishes. In addition, the effects of tissue culture surface, cell seeding density and FBS concentration with ascorbic acid treatment on specific gene expressions were determined. We believe that H9C2 cardiomyoblast cell sheets obtained with ascorbic acid treatment with 100 μg/mL AA in the presence of high cell density (5×10^4 cells/cm^2) and high serum content (20% FBS) can be a good in vitro model for heart disease and cardiac tissue engineering studies.

Acknowledgements This study was financially supported by The Hacettepe University Scientific Research Projects Coordination Unit Project No. FBA-2017-16248. The authors would like to thank Selin Gümüşderelioğlu for English editing of text language.

Compliance with ethical standards

Conflict of interest The authors declare that they have no conflict of interest.

References

Bel A, Planat-Bernard V, Saito A, Bonnevie L, Bellamy V et al (2010) Composite cell sheets: a further step toward safe and effective myocardial regeneration by cardiac progenitors derived from embryonic stem cells. Circulation 122:118–123

Chen CH, Chang Y, Wang CC, Huang CH, Huang CC, Yeh YC, Hwang SM, Sung HW (2007) Construction and characterization of fragmented mesenchymal-stem-cell sheets for intramuscular injection. Biomaterials 28:4643–4651

Choi YC, Morris GM, Lee FS, Sokoloff L (1980) The effect of serum on monolayer cell culture of mammalian articular chondrocytest. Connect Tissue Res 7:105–112

Cui H, Liu Y, Cheng Y, Zhang Z, Zhang P, Chen X, Wei Y (2014) In vitro study of electroactive tetraaniline-containing thermosensitive hydrogels for cardiac tissue engineering. Biomacromolecules 15:1115–1123

Cui H, Miao S, Esworthy T, Zhou X, Lee S-J, Liu C, Yu Z-X, Fisher JP, Mohiuddin M, Zhang LG (2018) 3D bioprinting for cardiovascular regeneration and pharmacology. Adv Drug Deliv Rev 132:252–269

Dergilev KV, Makarevich PI, Tsokolaeva ZI, Boldyreva MA, Beloglazova IB, Zubkova ES, Menshikov MY, Parfyonova YV (2017) Comparison of cardiac stem cell sheets detached by Versene solution and from thermoresponsive dishes reveals similar properties of constructs. Tissue Cell 49:64–71

Dergilev K, Tsokolaeva Z, Makarevich P, Beloglazova I, Zubkova E, Boldyreva M, Ratner E, Dyikanov D, Menshikov M, Ovchinnikov A, Ageev F, Parfyonova Y (2018) C-kit cardiac progenitor cell based cell sheet improves vascularization and attenuates cardiac remodeling following myocardial infarction in rats. BioMed Res Int 2018, 3536854. https://doi.org/10.1155/2018/3536854

Dott W, Mistry P, Wright J, Cain K, Herbert KE (2014) Modulation of mitochondrial bioenergetics in a skeletal muscle cell line model of mitochondrial toxicity. Redox Biol 2:224–233

Feridooni T, Mac Donald C, Shao D, Yeung P, Agu RU (2013) Cytoprotective potential of anti-ischemic drugs against chemotherapy-induced cardiotoxicity in H9C2 myoblast cell line. Acta Pharm 63:493–503

Furuta A, Miyoshi S, Itabashi Y, Shimizu T, Kira S et al (2006) Pulsatile cardiac tissue grafts using a novel three-dimensional cell sheet manipulation technique functionally integrates with the host heart, in vivo. Circ Res 98:705–712

Grinnell F, Fukamizu H, Pawelek P, Nakagawa S (1989) Collagen processing, crosslinking, and fibril bundle assembly in matrix produced by fibroblasts in long-term cultures supplemented with ascorbic acid. Exp Cell Res 181:483–491

Guo P, Zeng JJ, Zhou N (2015) A novel experimental study on the fabrication and biological characteristics of canine bone marrow mesenchymal stem cells sheet using vitamin C. Scanning 37:42–48

Hakimi O, Poulson R, Thakkar D, Yapp C, Carr A (2014) Ascorbic acid is essential for significant collagen deposition by human tenocytes *in vitro*. Oxid Antioxid Med Sci 3:119–127

Haraguchi Y, Shimizu T, Yamato M, Kikuchi A, Okano T (2006) Electrical coupling of cardiomyocyte sheets occurs rapidly via functional gap junction formation. Biomaterials 27:4765–4774

Haraguchi Y, Shimizu T, Sasagawa T, Sekine H, Sakaguchi K et al (2012) Fabrication of functional three-dimensional tissues by stacking cell sheets *in vitro*. Nat Protoc 7:850–858

Hata H, Matsumiya G, Miyagawa S, Kondoh H, Kawaguchi N et al (2006) Grafted skeletal myoblast sheets attenuate myocardial remodeling in pacing-induced canine heart failure model. J Thorac Cardiovasc Surg 132:918–924

Hoashi T, Matsumiya G, Miyagawa S, Ichikawa H, Ueno T et al (2009) Skeletal myoblast sheet transplantation improves the diastolic function of a pressure-overloaded right heart. J Thorac Cardiovasc Surg 138:460–467

Hong Y, Yu M, Weng W, Cheng K, Wang H, Lin J (2013) Light-induced cell detachment for cell sheet technology. Biomaterials 34:11–18

Huang CH, Chen HW, Tsai MS, Hsu CY, Peng RH et al (2009) Antiapoptotic cardioprotective effect of hypothermia treatment against oxidative stress injuries. Acad Emerg Med 16:872–880

Itabashi Y, Miyoshi S, Kawaguchi H, Yuasa S, Tanimoto K et al (2005) A New method for manufacturing cardiac cell sheets using fibrin-coated dishes and its electrophysiological studies by optical mapping. Artif Organs 29:95–103

Ivanyuk D, Budash G, Zheng Y, Gaspar JA, Chaudhari U et al (2015) Ascorbic acid-induced cardiac differentiation of murine pluripotent stem cells: transcriptional profiling and effect of a small molecule synergist of wnt/β-catenin signaling pathway. Cell Physiol Biochem 36:810–830

Jadaun P, Yadav D, Bisen PS (2018) Spirulina platensis prevents high glucose-induced oxidative stress mitochondrial damage mediated apoptosis in cardiomyoblasts. Cytotechnology 70:523–536

Kato S, Shanley JR, Fox JC (1996) Serum stimulation, cell-cell interactions, and extracellular matrix independently influence smooth muscle cell phenotype in vitro. Am J Pathol 149:687–697

Kawamura M, Miyagawa S, Miki K, Saito A, Fukushima S et al (2012) Feasibility, safety, and therapeutic efficacy of human induced pluripotent stem cell-derived cardiomyocyte sheets in a porcine ischemic cardiomyopathy model. Circulation 126:29–37

Kondoh H, Sawa Y, Miyagawa S, Sakakida-Kitagawa S, Memon IA et al (2006) Longer preservation of cardiac performance by sheet-shaped myoblast implantation in dilated cardiomyopathic hamsters. Cardiovasc Res 69:466–475

Koo MA, Lee MH, Kwon BJ, Seon GM, Kim MS, Kim D, Nam KC, Park JC (2018) Exogenous ROS-induced cell sheet transfer based on hematoporphyrin-polyketone film via a one-step process. Biomaterials 161:47–56

Law CH, Li JM, Chou HC, Chen YH, Chan HL (2013) Hyaluronic acid-dependent protection in H9C2 cardiomyocytes: a cell model of heart ischemia–reperfusion injury and treatment. Toxicology 303:54–71

Leung GP, Tse CM, Man RY (2007) Characterization of adenosine transport in H9C2 cardiomyoblasts. Int J Cardiol 116:186–193

L'Heureux N, Pâquet S, Labbé R, Germain L, Auger FA (1998) A completely biological tissue-engineered human blood vessel. FASEB J 12:47–56

Martinez EC, Wang J, Gan SU, Singh R, Lee CN, Kofidis T (2010) Ascorbic acid improves embryonic cardiomyoblast cell survival and promotes vascularization in potential myocardial grafts in vivo. Tissue Eng Part A 16:1349–1361

Matsuda N, Shimizu T, Yamato M, Okano T (2007) Tissue engineering based on cell sheet technology. Adv Mater 19:3089–3099

Mejia-Alvarez R, Tomaselli CF, Marban E (1994) Simultaneous expression of cardiac and skeletal muscle isoforms of the L-type Ca^{2+} channel in a rat heart muscle cell line. J Physiol 478:315–329

Memon IA, Sawa Y, Fukushima N, Matsumiya G, Miyagawa S et al (2005) Repair of impaired myocardium by means of implantation of engineered autologous myoblast sheets. J Thorac Cardiovasc Surg 130:1333–1341

Menard C, Pupier S, Mornet D, Kitzmann M, Nargeot J, Lory P (1999) Modulation of L-type calcium channel expression during retinoic acid-induced differentiation of H9C2 cardiac cells. J Biol Chem 274:29063–29070

Miyahara Y, Nagaya N, Kataoka M, Yanagawa B, Tanaka K et al (2006) Monolayered mesenchymal stem cells repair scarred myocardium after myocardial infarction. Nat Med 12:459–465

Narayanan AS, Page RC, Swanson J (1989) Collagen synthesis by human fibroblasts regulation by transforming growth factor-β in the presence of other inflammatory mediators. Biochem J 260:463–469

Pereira SL, Ramalho-Santos J, Branco AF, Sardão VA, Oliveira PJ, Carvalho RA (2011) Metabolic remodeling during H9C2 myoblast differentiation: relevance for in vitro toxicity studies. Cardiovasc Toxicol 11:180–190

Ricotti L, Polini A, Genchi GG, Ciofani G, Iandolo D et al (2012) Proliferation and skeletal myotube formation capability of C2C12 and H9c2 cells on isotropic and anisotropic electrospun nanofibrous PHB scaffolds. Biomed Mater 7, 035010. https://doi.org/10.1088/1748-6041/7/3/035010

Rodgers BD, Interlichia JP, Garikipati DK, Mamidi R, Chandra M et al (2009) Myostatin represses physiological hypertrophy of the heart and excitation–contraction coupling. J Physiol 587:4873–4886

Sekine H, Shimizu T, Hobo K, Sekiya S, Yang J et al (2008) Endothelial cell coculture within tissue-engineered cardiomyocyte sheets enhances neovascularization and improves cardiac function of ischemic hearts. Circulation 118:145–152

Sekine H, Shimizu T, Dobashi I, Matsuura K, Hagiwara N et al (2011) Cardiac cell sheet transplantation improves damaged heart function via superior cell survival in comparison

with dissociated cell ınjection. Tissue Eng Part A 17:2973–2980

Shimizu K, Ito A, Lee JK, Yoshida T, Miwa K et al (2007) Construction of multi-layered cardiomyocyte sheets using magnetite nanoparticles and magnetic force biotechnology and bioengineering. Biotechnol Bioeng 96:803–809

Tao H, Nuo M, Min S (2018) Sufentanil protects the rat myocardium against ischemia–reperfusion injury via activation of the ERK1/2 pathway. Cytotechnology 70:169–176

Watkins SJ, Borthwick GM, Arthur HM (2011) The H9C2 cell line and primary neonatal cardiomyocyte cells show similar hypertrophic responses in vitro. Vitro Cell Dev Biol Anim 47:125–131

Wei FL, Qu CY, Song TL, Ding G, Fan ZP et al (2012) Vitamin C treatment promotes mesenchymal stem cell sheet formation and tissue regeneration by elevating telomerase activity. J Cell Physiol 227:3216–3224

Witek P, Korga A, Burdan F, Ostrowska M, Nosowska B et al (2016) The effect of a number of H9C2 rat cardiomyocytes passage on repeatability of cytotoxicity study results. Cytotechnology 68:2407–2415

Yamato M, Okano T (2004) Cell sheet engineering. Mater Today 7:42–47

Yeh TS, Fang YHD, Lu CH, Chiu SC, Yeh CL et al (2014) Baculovirus-transduced, VEGF-expressing adipose-derived stem cell sheet for the treatment of myocardium infarction. Biomaterials 35:174–184

Yu J, Tu YK, Tang YB, Cheng NC (2014) Stemness and transdifferentiation of adipose-derived stem cells using L-ascorbic acid 2-phosphate-induced cell sheet formation. Biomaterials 35:3516–3526

Zahn R, Thomasson E, Guillaume-Gentil O, Vörös J, Zambelli T (2012) Ion-induced cell sheet detachment from standard cell culture surfaces coated with polyelectrolytes. Biomaterials 33:3421–3427

Zhang H, Yu N, Zhou Y, Ma H, Wang J et al (2016) Construction and characterization of osteogenic and vascular endothelial cell sheets from rat adipose-derived mesenchymal stem cells. Tissue Cell 48:488–495

Zhou T, Zhou Z, Zhou S, Huang F (2016) Real-time monitoring of contractile properties of H9C2 cardiomyoblasts by using a quartz crystal microbalance. Anal Methods 8:488–495